Line Correspondences Between Two Images Using Local Affine Moment Invariant

C.H. Chan, Y.S. Hung and C.H. Leung
Department of Electrical and Electronic Engineering
The University of Hong Kong, Pokfulam Road, Hong Kong, P.R.China
{chchan, yshung, chleung}@eee.hku.hk

ABSTRACT

This paper proposes an algorithm for matching line segments between two images which are related by affine transformations using local affine moment invariant (AMI). Instead of using traditional methods for objection recognition in which each object is **globally** represented by a vector of affine moment invariants, here each pair of line segments extracted from each image is **locally** represented by an affine moment invariant. This algorithm is suitable for line correspondences with multi-planes and occlusion. Matches are determined through comparing invariant values and voting. Experimental results are given for both synthetic and real images. The noise model of affine moment invariant is also presented.

Keywords

Affine transformation, Line matching, Local affine moment invariant (AMI)

1. INTRODUCTION

Image matching is one of the basic problems in computer vision. It is the process of finding features such as line segments in different images that represent the same feature of the observed scene. Many papers have been published in the past on line matching under an affine transformation. Some of them make use of geometric invariants for matching. Lamdan *et.al* [Lam90a] developed a geometric hashing technique which calculates affine invariant coordinates for arbitrary point sets under various geometric transformations. The method is however very computation intensive. There are three other commonly used affine invariants: distance ratio [Hut91a], area ratio [Cha02a], and affine moment invariant (AMI) [Flu94a]. Distance ratio and area ratio are ratios of two relative affine invariants, so they may have an ordering problem. On the other hand, AMI is defined over an area and is invariant to the starting position. Besides, AMI is more robust to noise. Figure 1 shows the average error (in %) of the invariants against the noise level (in *SNR*) on 1000 arbitrary quadrangles. The upper one is area ratio, the middle one is distance ratio and the bottom one is AMI. It can be seen that AMI can tolerate a larger range of noise.

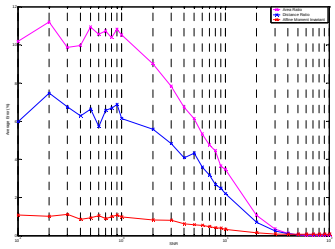

Figure 1. Robustness of different invariants to noise.

All methods which use AMIs, to the best of our knowledge, are mainly for pattern matching or object recognition. They are computed over a set of data points or a closed-boundary region (usually an object), so they may encounter the problem of occlusion. Distance ratio and area ratio have been proposed by some authors for localized line matching [Gro95a], but AMIs have not been used for the same purpose. This paper presents the key idea to match line segments between two affine transformed images using local AMI. The noise model of AMI is also presented.

2. ALGORITHM

2.1 Selection of line segments

This algorithm assumes that both images contain line segments that do not intersect except at their end points only. In the case that there are intersecting lines, they are broken up so that finally there are only

WSCG 2005 SHORT papers proceedings, ISBN 80-903100-9-5
WSCG'2005, January 31-February 4, 2005
Plzen, Czech Republic.

two kinds of line configurations: connected lines (3 noncollinear point pairs) and disjoint lines (4 noncollinear point pairs). Since connected lines provide just enough information to determine the affine transformation, even if the point pairs are mismatched, we can still find a transformation which can exactly relate the point pairs. Hence, such configuration does not help line matching at all. On the other hand, for disjoint lines, besides 3 basic point pairs, there is one extra point pair which enforces an extra constraint for the determination of an affine transformation. There is no exact solution except when all 4 pairs are really related by an affine transformation. Since such configuration has a discriminatory power, this algorithm only considers line matching based on the affine moment invariant calculated from such configuration.

2.2 Selection of starting position

Given a pair of disjoint lines in both images, the end point correspondences are not known, so there are 4! = 24 combinations of end point correspondence. To reduce the number of combinations, the convex hull constraints are added. Hartley proved that projective transformation preserves the convex hull of a point set [Har93a]. In the four-point case, the convex hull may contain 3 or 4 points.

First consider the convex hull containing all 4 points, we can form a loop which passes through the end points one by one with no skipping as shown below.

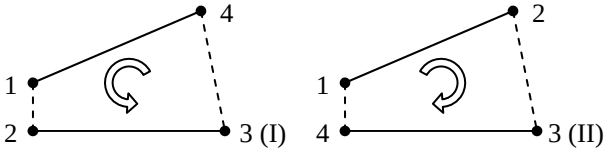

Figure 2. Convex hull containing 4 points.

If the conditions above are enforced, the number of combinations is reduced to 8 (4 clockwise and 4 anti-clockwise). If the orientation of the convex hull is chosen for all pairs of lines in both images to be in clockwise direction, the number of combinations is reduced to 4. Finally, the loop can be restricted to traverse both points of one line segment before going on to another line segment, whereby the number of combinations is reduced to 2. For example, in diagram (II) above, the only possible loops are either (1→2→3→4) or (3→4→1→2).

Now consider the convex hull containing only 3 points as shown in Figure 3. If the same rules are applied, four combinations are valid: (1→2→3→4), (2→1→3→4), (3→4→1→2) and (3→4→2→1). Note that the relative size of areas is preserved under an affine transformation, i.e., if area A is larger than area B in the first image, the affine transformed area A is still larger than the transformed area B in the transformed image. Hence, the number of loops is reduced by half if they are restricted to have a larger area. If the area enclosed by the path (1→2→3→4) or (3→4→1→2) is larger than that enclosed by the path (3→4→2→1) or (2→1→3→4), then paths (1→2→3→4) and (3→4→1→2) are selected.

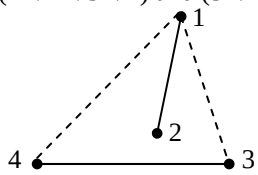

Figure 3. Convex hull containing 3 points.

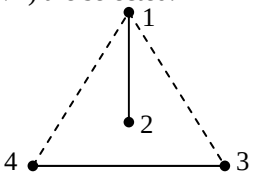

Figure 4. Symmetric line pattern.

In the case that the line pattern is symmetric as shown in Figure 4, there is an ambiguity in choosing the paths as the same area is enclosed by 4 different paths. However, the shape enclosed by the path (1→2→3→4) or (3→4→1→2) is just the reflection of the shape enclosed by the other two paths, and AMI is invariant to an affine transformation including reflection. Therefore, the AMIs for both areas are the same and can be used for matching.

2.3 Affine moment invariant

A moment invariant is a moment-based descriptor of a planar shape, and is very useful for pattern recognition. J. Flusser and T. Suk extended the idea to AMI, which is invariant under an affine transformation [Flu93a]. The moment $m(p,q)$ of order $(p + q)$ of a binary 2-D object G is defined as:

$$m(p,q) = \iint_G x^p y^q \, dx \, dy \quad \ldots (1)$$

while the central moment $\mu(p,q)$ of order $(p + q)$ is defined as:

$$\mu(p,q) = \iint_G (x - x_t)^p (y - y_t)^q \, dx \, dy \ldots (2)$$

where $x_t = m_{10}/m_{00}$ and $y_t = m_{01}/m_{00}$ are the coordinates of the center of gravity of object G. The second-order AMI is defined as [Flu94a]:

$$AMI = \frac{1}{\mu(0,0)^4}(\mu(2,0)\mu(0,2) - \mu(1,1)^2) \quad \ldots (3)$$

It is a time consuming task to compute the double integrals of equations (1) and (2). Our algorithm is based on the method described in [Sin93a]. In order to use AMI for line matching, we need to derive the variance of AMI when the line segments are perturbed by noise. Assume we are given 4 ordered points (x_i, y_i), $i = 0,\ldots,3$, which form the object G. Let $(p_1,\ldots,p_4,p_5,\ldots,p_8) = (x_0,\ldots,x_3,y_0,\ldots,y_3)$, and AMI = $f(p_1,\ldots,p_8)$, each variable p_i can be expressed as $p_i = \bar{p}_i + \delta_i$, where $\bar{p}_i$ is the true but unknown value of p_i , and δ_i is a random perturbation (noise) added to the true variable $\bar{p}_i$. Assume δ_i is independent and identically distributed with zero mean and standard deviation σ_δ. Then AMI = $f(\bar{p}_i + \delta_i; i = 1,...,8)$. Expanding AMI in Taylor series and neglect second and higher order terms:

$$AMI = f(\bar{p}_1,...,\bar{p}_8) + \sum_{i=1}^{8}\left[\delta_i \frac{\partial}{\partial \bar{p}_i} f(\bar{p}_1,...,\bar{p}_8)\right] \ldots(4)$$

Let $\bar{P} = (\bar{p}_1,...,\bar{p}_8)$, $\quad E[AMI] = f(\bar{P}) \ldots(5)$

$$\sigma_{AMI}^2 = E[(AMI - E(AMI))^2] = \sigma_\delta^2 \sum_{i=1}^{8}\left(\frac{\partial}{\partial \bar{p}_i} f(\bar{P})\right)^2 \ldots(6)$$

Let $g(\bar{P}) = \dfrac{m(2,0)m(0,2) - m(1,1)^2}{m(0,0)^4} \ldots(7)$,

From(3), $f(\bar{P}) = g(\bar{x}_i - \bar{x}_t, \bar{y}_i - \bar{y}_t; i = 0,...,3)$, where $(\bar{x}_t, \bar{y}_t)$ are the coordinates of the center of gravity of object G without noise. Let $X_i = \bar{x}_i - \bar{x}_t$; $Y_i = \bar{y}_i - \bar{y}_t$, each term in (6) can be computed as follows:

$$\frac{\partial f}{\partial \bar{x}_i} = \frac{\partial g(X_i, Y_i; i = 0,...,3)}{\partial X_i} \ldots(8); \quad \frac{\partial f}{\partial \bar{y}_i} = \frac{\partial g(X_i, Y_i; i = 0,...,3)}{\partial Y_i} \ldots(9)$$

$$\frac{\partial g}{\partial X_i} = \frac{1}{m(0,0)^4}\left[m(2,0)\frac{\partial m(0,2)}{\partial X_i} + m(0,2)\frac{\partial m(2,0)}{\partial X_i} - 2m(1,1)\frac{\partial m(1,1)}{\partial X_i}\right] - 4\frac{m(2,0)m(0,2) - m(1,1)^2}{m(0,0)^5}\frac{\partial m(0,0)}{\partial X_i}$$

$$\frac{\partial g}{\partial Y_i} = \frac{1}{m(0,0)^4}\left[m(2,0)\frac{\partial m(0,2)}{\partial Y_i} + m(0,2)\frac{\partial m(2,0)}{\partial Y_i} - 2m(1,1)\frac{\partial m(1,1)}{\partial Y_i}\right] - 4\frac{m(2,0)m(0,2) - m(1,1)^2}{m(0,0)^5}\frac{\partial m(0,0)}{\partial Y_i}$$

$$\frac{\partial m(0,2)}{\partial X_i} = \frac{1}{12}\left[Y_{i+1}\left(Y_i^2 + Y_i Y_{i+1} + Y_{i+1}^2\right) - Y_{i-1}\left(Y_{i-1}^2 + Y_{i-1}Y_i + Y_i^2\right)\right]$$

$$\frac{\partial m(2,0)}{\partial X_i} = \frac{1}{12}\left[(X_{i-1} + X_i)^2(Y_i - Y_{i-1}) + (X_i + X_{i+1})^2(Y_{i+1} - Y_i) + 2X_i^2(Y_{i+1} - Y_{i-1})\right]$$

$$\frac{\partial m(1,1)}{\partial X_i} = \frac{1}{12}\left[Y_{i+1}^2(X_i + X_{i+1}) + Y_i^2(X_{i-1} - X_{i+1}) - Y_{i-1}^2(X_{i-1} + X_i) - 2X_i Y_i(Y_{i-1} - Y_{i+1})\right]$$

$$\frac{\partial m(0,0)}{\partial X_i} = \frac{1}{2}[Y_{i+1} - Y_{i-1}]; \qquad \frac{\partial m(0,0)}{\partial Y_i} = \frac{1}{2}[X_{i-1} - X_{i+1}]$$

$$\frac{\partial m(0,2)}{\partial Y_i} = \frac{1}{12}\left[(Y_{i-1} + Y_i)^2(X_{i-1} - X_i) + (Y_i + Y_{i+1})^2(X_i - X_{i+1}) + 2Y_i^2(X_{i-1} - X_{i+1})\right]$$

$$\frac{\partial m(2,0)}{\partial Y_i} = \frac{1}{12}\left[X_{i-1}\left(X_{i-1}^2 + X_{i-1}X_i + X_i^2\right) - X_{i+1}\left(X_i^2 + X_i X_{i+1} + X_{i+1}^2\right)\right]$$

$$\frac{\partial m(1,1)}{\partial Y_i} = \frac{1}{12}\left[X_{i-1}^2(Y_{i-1} + Y_i) - X_i^2(Y_{i-1} - Y_{i+1}) - X_{i+1}^2(Y_i + Y_{i+1}) + 2X_i Y_i(X_{i-1} - X_{i+1})\right]$$

2.4 Procedure

This subsection describes the whole procedure of line matching in details. Given *M* and *N* line segments extracted from two images which are approximately related by unknown affine transformations, the matching procedure consists of the following steps:

2.4.1 Step 1

Construct connectivity tables of size *M*×*M* and *N*×*N* for the first and second images respectively. These tables show if segments are connected to the starting or end points of other line segments in the image.

2.4.2 Step 2

Construct affine moment invariant tables of size *M*×*M* and *N*×*N* for the first and second images respectively. In the calculation of the affine moment invariant between two segments, a path through the line segments is chosen such that the line configuration fulfills the requirement described in section 2.2. Besides, given the standard deviation of noise σ_δ, the range for each affine moment invariant (AMI $\pm$ σ_{AMI}) is computed. In the case that two line segments are found to be connected from the previous step, they will not be considered in the following steps.

2.4.3 Step 3

Each affine moment invariant in the moment invariant table for the first image is compared with all invariants of the second image. If the affine moment invariant between two line segments in the second image is within the range of the invariant (defined by the standard deviation of noise σ_δ) between two line segments in the first image, the pairs of segments are regarded as a putative match which is then verified as follows. Since they are arranged in the configuration described in section 2.2, each pair of line segments would only have 2 possible paths. Therefore, by calculating the two affine transformations and projecting the two line segments in the first image into the second image, the average projection error for each transformation is found. If the smaller of the two errors is less than a predefined threshold, then the pairs of line segments are regarded as matched with known segment correspondences.

Next, form a voting table of size *M*×*N*. A vote is added to each of the (*i*,*k*) and (*j*,*l*) cells of the vote table if the segment pair (*i*,*j*) in the first image is matched to (*k*,*l*) in the second image. This table accumulates the number of votes for line correspondences between the two images. The higher the number of votes, the higher the possibility that the corresponding line segments are matched.

Besides, form an ordering table of size *M*×*M* and *N*×*N* for the first and second images. As described above, each line segment may change its vertex order such that it fulfills the requirement described in section 2.2. The vertex ordering information is stored in the ordering tables. The (*i*,*j*) entry states whether the line segment *i* needs to change its vertex order when pairing up with the line segment *j*.

The ordering information is entered into the ordering tables only when the pair of line segments has found a match during comparison, i.e. the projection error is less than the predefined threshold.

2.4.4 Step 4

Given the vote table formed from Step 3, the final matches between the two images are determined. A winner-takes-all approach is adopted.

2.4.5 Step 5

After a set of line matches are found from Step 4, the end point correspondences are performed. For each matched line segment, by examining the ordering information of all other matched line segments which have been paired with it, we can deduce the correct sense of direction of the line segment in a

correspondence.

2.5 Improving line matching

There are other finer data available to improve the validity of computed matches and possibly to find new ones. One such information is the connectivity. If two line segments are connected in the first image, the corresponding line segments in the second image should also be connected. Moreover, the sense of direction of the segments relative to the connected vertex should be consistent.

3. EXPERIMENTAL RESULTS

In this section, the algorithm is tested using 2 sets of images. The first set is a pair of images of a planar object as shown in Figure 5. Both images contain 68 line segments with noise.

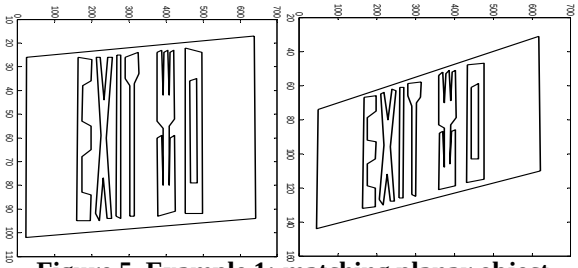

Figure 5. Example 1: matching planar object.

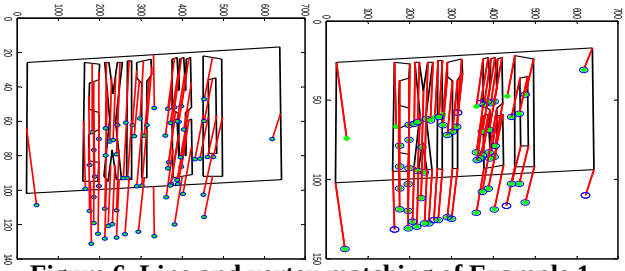

Figure 6. Line and vertex matching of Example 1.

Figure 6 shows the matching results. The left figure shows the vector flows between the mid-points of matched line segments superimposed on the first image. Each flow is a match and the dot represents the mid-point of the corresponding line segment in the second image. In this example, all line matches are correct. The right figure shows the vector flows of vertex matching superimposed on the first image. As each line segment has two vertices, the first vertex is represented by a solid dot while the second vertex is represented by a circle. In this example, all vertices are correctly matched.

Figure 7 shows a pair of images with multi-planes. The edges are approximated by noisy line segments in the two images that may not correspond. The first image contains 122 line segments and the second has 93. Figure 8 shows the matching results. 91 line segments (182 vertices) are matched, with 13 (resp. 26 vertices) mismatches. The main reason for the mismatches is that the series of windows at the bottom of the images in Figure 7 are very similar and errors often occur in such situations.

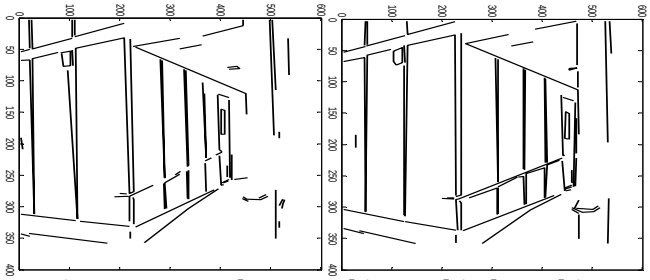

Figure 7. Example 2: matching multi-plane objects.

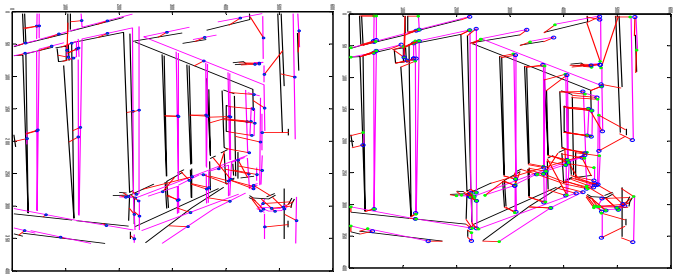

Figure 8. Line and vertex matching of Example 2.

4. CONCLUSION

The algorithm for line matching between two images related by affine transformations is developed, which is based on the matching of local second-order affine moment invariants. Experimental results are presented which show the applicability to multi-planes line matching with noise.

5. ACKNOWLEDGMENTS

The work described in this paper was supported by a grant from the Research Grants Council of Hong Kong SAR, China (Project No.HKU7058/02E) and partially by CRCG of the University of Hong Kong.

6. REFERENCES

[Cha02a] H. B. Chan and Y. S. Hung, “Matching patterns of line segments by eigenvector decomposition”, SSIAI’02, pp. 286-289, 2002.

[Flu93a] J. Flusser and T. Suk, “Pattern recognition by affine moment invariants”, Pattern Recognition, vol. 26, pp. 167-174, 1993.

[Flu94a] J. Flusser and T. Suk, “A moment-based approach to registration of images with affine geometric distortion”, IEEE Transactions on Geoscience and Remote Sensing, vol. 32, no. 2, March, 1994.

[Gro95a] P. Gros, O. Bournez, and E. Boyer, “Using geometric quasi-invariants to match and model images of line segments”, research report INRIA, No2608, July 1995.

[Har93a] R. Hartley, “Cheirality invariants”, In Proc. of DARPA Image Understanding Workshop, Washington, D. C., pp. 745-753, 1993.

[Hut91a] D. P. Huttenlocher, “Fast affine point matching: An output-sensitive method”, CVPR91, pp. 263-268.

[Lam90a] Y. Lamdan, J. Schwartz, and H. Wolfson, “Affine invariant model-based object recognition”, IEEE Trans. Robotics and Automation, vol. 6, No. 5, pp. 578-589, 1990.

[Sin93a] Mark H. Singer, “A general approach to moment calculation for polygons and line segments”, Pattern Recognition, vol. 26, No. 7, pp. 1019-1028, 1993.